Cellular/Molecular

$P2X_4$ Receptors Influence Inflammasome Activation after Spinal Cord Injury

Juan Pablo de Rivero Vaccari,[1]* Dominic Bastien,[4]* Geoffrey Yurcisin,[2] Isabelle Pineau,[4] W. Dalton Dietrich,[1] Yves De Koninck,[3] Robert W. Keane,[1,2] and Steve Lacroix[4]

[1]The Miami Project to Cure Paralysis and [2]Department of Physiology and Biophysics, University of Miami Miller School of Medicine, Miami, 33136, Florida, [3]Institut Universitaire de Santé Mentale de Québec, Québec, Canada, G1J 2G3, and [4]Centre de Recherche du Centre Hospitalier de l'Université Laval and Department of Molecular Medicine, Université Laval, Québec, Québec, Canada, G1V 4G2

$P2X_4$ and $P2X_7$ are the predominant purinergic P2X receptor subtypes expressed on immune and neural cells. These receptor subtypes traffic between intracellular compartments and the plasma membrane and form protein interactions with each other to regulate ATP-dependent signaling. Our recent studies have shown that $P2X_7$ receptors in neurons and astrocytes activate NLRP1 inflammasomes, but whether $P2X_4$ receptors regulate inflammasome signaling is essentially unknown. Here, we demonstrate that $P2X_4$ receptors are expressed in neurons of the spinal cord. We provide direct evidence that spinal cord injury (SCI) induces an innate inflammatory response that leads to increased caspase-l cleavage and production of IL-1β but not IL-18. Consistent with these findings, $P2X_4$ knock-out mice showed impaired inflammasome signaling in the cord, resulting in decreased levels of IL-1β and reduced infiltration of neutrophils and monocyte-derived M1 macrophages, resulting in significant tissue sparing and improvement in functional outcomes. These results indicate that $P2X_4$ receptors influence inflammasome signaling involving caspase-1 activation and IL-1β processing in neurons after SCI. $P2X_4$ might thus represent a potential therapeutic target to limit inflammatory responses associated with SCI and neurodegenerative disorders.

Introduction

The innate immune response is classically known as the first line of defense against endogenous and exogenous insults. However, innate immunity actually serves as a sophisticated system for sensing "danger signals," such as host-derived signals of cellular stress and tissue destruction. One of the most studied endogenous insults that activates the innate immune response is ATP. Extracellular ATP is elevated in neuroinflammation in spinal cord injury (SCI) and neuropathic pain and acts on purinergic receptors such as $P2X_7$ or $P2X_4$ (Tsuda et al., 2003; Wang et al., 2004; Coull et al., 2005). $P2X_4$ is the most abundant P2X receptor subtype present in the CNS (Buell et al., 1996; Soto et al., 1996). It is expressed in neurons of different brain regions and in microglia (Burnstock, 2007; Ulmann et al., 2008).

Increased expression of $P2X_4$ is observed in injured tissue after SCI (Schwab et al., 2005), traumatic brain injury (Zhang et al., 2006), and cerebral ischemia (Cavaliere et al., 2003). Moreover, $P2X_4$ receptors are elevated in spinal cord microglia after peripheral nerve injury (Tsuda et al., 2003; Ulmann et al., 2008). Neutralizing $P2X_4$ activity using an antisense oligonucleotide or a transgenic approach prevents tactile allodynia (Tsuda et al., 2003; Ulmann et al., 2008), suggesting that $P2X_4$ receptors are involved in neuropathic pain. $P2X_4$ receptors are also expressed within the immune system (Wang et al., 2004). However, the involvement of $P2X_4$ in neuroinflammatory processes remains unresolved.

The inflammasome is a multiprotein complex that promotes the maturation of inflammatory cytokines, such as IL-1β and IL-18, and is therefore likely to control many aspects of neuroinflammatory processes. Our previous work demonstrated that $P2X_7$ receptors activate the NLRP1 inflammasome in neurons and astrocytes via a mechanism mediated by pannexin-1 (Silverman et al., 2009). Heteromeric interactions between $P2X_4$ and $P2X_7$ receptors have been reported in human embryonic kidney 293 cells and in primary cultures of bone marrow-derived macrophages (Guo et al., 2007; Casas-Pruneda et al., 2009). Moreover, genetic knockdown studies in mouse epithelial cells indicate that interactions between $P2X_4$ and $P2X_7$ regulate overall P2X receptor levels (Weinhold et al., 2010). In this study, we used $P2X_4$ knock-out (KO) mice to examine the role of $P2X_4$ receptors in inflammasome activation and neuroinflammation after SCI. We show that $P2X_4$-KO mice have significant decreases in inflammasome activation, proinflammatory cytokine production, inflammatory cell infiltration, and improved histopathological and functional outcomes compared with wild types (WTs) after

Received Sept. 27, 2011; revised Dec. 15, 2011; accepted Jan. 9, 2012.

Author contributions: J.P.d.R.V., R.W.K., and S.L. designed research; J.P.d.R.V., D.B., G.Y., I.P., R.W.K., and S.L. performed research; W.D.D., Y.d.K., R.W.K., and S.L. contributed unpublished reagents/analytic tools; J.P.d.R.V., D.B., R.W.K., and S.L. analyzed data; J.P.d.R.V., R.W.K., and S.L. wrote the paper.

This study was supported by Canadian Institutes of Health Research Grant MOP-84558 (S.L.) and National Institutes of Health Grant NS059836 and Craig Nielsen Foundation Grant 124671 (R.W.K.) S. L. is supported by the Fonds de la Recherche en Santé du Québec. We thank Nicolas Vallières, Nadia Fortin, and Karen Vandal for their invaluable technical assistance. We are also grateful to Dr. Armen Saghatelyan (Centre de Recherche Université Laval Robert-Giffard, Québec, QC, Canada) for giving us access to his laser scanning confocal microscope.

*J.P.d.R.V. and D.B. contributed equally to this work.

Correspondence should be addressed to Dr. Steve Lacroix, Centre Hospitalier de l'Université Laval Research Center, 2705, Boulevard Laurier, Québec, QC, Canada, G1V 4G2. E-mail: Steve.Lacroix@crchul.ulaval.ca.

DOI:10.1523/JNEUROSCI.4930-11.2012

 0270-6474/12/323058-09$15.00/0

SCI. Thus, $P2X_4$ receptors may play a critical role in neurons mediating innate neuroinflammatory events after SCI.

Materials and Methods

Animals. A total of 190 adult mice of either sex were used in this study. $P2X_4$-KO mice in the C57BL/6 background were generated, reproduced, and genotyped as described previously by the Rassendren laboratory (Ulmann et al., 2008). C57BL/6 mice from Charles River Laboratories were used as controls. Bone marrow chimeric mice were produced using our previously published protocol (Pineau and Lacroix, 2007). All mice had access to food and water *ad libitum*.

SCI. C57BL/6 ($n = 99$) and $P2X_4$-KO ($n = 91$) mice were anesthetized with isoflurane and underwent a laminectomy at vertebral level T9–T10, which corresponds to spinal segment T10–T11. Briefly, the vertebral column was stabilized, and a contusion of 70 kdyn was performed using the Infinite Horizon SCI device (Precision Systems and Instrumentation). Animals used for behavioral testing received a 50 kdyn injury. Overlying muscular layers were then sutured and cutaneous layers were stapled. Postoperatively, animals received manual bladder evacuation twice daily to prevent urinary tract infections. Depending on the experiment performed, SCI mice were killed at 30 min, 6 and 12 h, and 3, 4, 7, 14, and 38 d after contusion. All surgical procedures were approved by the Laval University Animal Care Committee and followed Canadian Council on Animal Care guidelines.

Immunoblotting. For detection of protein levels, a 4 mm spinal cord segment centered over the lesion was harvested at different time points after injury with extraction buffer (20 mM Tris-HCl, pH 7.5, 150 mM NaCl, 1% Triton X-100, 1 mM EDTA acid, 1 mM EGTA, 2.5 mM pyrophosphate, and 1 mM β-glycerophosphate) containing protease and phosphatase inhibitor cocktails (Sigma). Immunoblot analysis was performed with the Criterion system (Bio-Rad), as described previously (de Rivero Vaccari et al., 2008), using antibodies to caspase-1 (1:1000; Imgenex), IL-1β (1:10,000; National Cancer Institute), IL-18 (1:1000; Abcam), $P2X_4$ (1:1000; Abcam), and $P2X_7$ (1:1000; Alomone Labs). Actin (Sigma, 1:10,000) was used as a protein loading control and internal standard.

Flow cytometry. Cells freshly isolated from the spinal cord of injured mice were analyzed using flow cytometry following our previously published method (Pineau et al., 2010). Briefly, animals were transcardially perfused with cold HBSS to remove immune cells from the vasculature, their spinal cords were dissected out, and a 1 cm segment centered at the site of the lesion was isolated and mechanically homogenized with a small tissue grinder. Cells were filtered through a 40 μm nylon mesh cell strainer (BD Biosciences), centrifuged at 200 $\times$ *g* for 10 min, washed once with HBSS, and resuspended with HBSS containing 20% fetal bovine serum (Sigma-Aldrich). For multicolor immunofluorescent labeling, cells were incubated with Mouse Fc Block (i.e., purified anti-mouse CD16/CD32; BD Biosciences) for 5 min to prevent nonspecific binding, followed by labeling for 30 min at room temperature with the following fluorescently conjugated primary antibodies: PerCP-conjugated anti-CD45 (1:33; BD Biosciences), BD Horizon V450-conjugated anti-CD11b (1:66; BD Biosciences), FITC-conjugated anti-Ly-6C (1:100; BD Biosciences), PE-Cy7-conjugated anti-Ly-6G (1:100; BD Biosciences), and PE-conjugated anti-7/4 (1:20; AbD Serotec) (for a full description of these primary antibodies, see Nadeau et al., 2011). Cells were analyzed using FlowJo software (version 9.2; Tree Star) on a FACS LSRII flow cytometer (BD Biosciences). Myeloid cells were identified based on their expression of CD45, CD11b, Ly-6C, and Ly-6G, as follows: neutrophils, $CD45^{hi}$ $CD11b^{+}$ $Ly\text{-}6C^{+}$ $Ly\text{-}6G^{+}$; monocyte-derived M1 macrophages, $CD45^{hi}$ $CD11b^{+}$ $Ly\text{-}6C^{hi}$ $Ly\text{-}6G^{-}$; monocyte-derived M2 macrophages, $CD45^{hi}$ $CD11b^{+}$ $Ly\text{-}6C^{-}$ $Ly\text{-}6G^{-}$; and microglia, $CD45^{dim}$ $CD11b^{+}$ $Ly\text{-}6C^{-}$ $Ly\text{-}6G^{-}$ (Babcock et al., 2003; Gordon and Taylor, 2005; Auffray et al., 2007; Nahrendorf et al., 2007). Also, the phenotype of these myeloid cells was analyzed by flow cytometry using antibodies directed against the following antigens: anaphase protein complex-conjugated anti-CD11c (1:50; BD Biosciences), Alexa Fluor 700-conjugated anti-major histocompatibility complex II (MHCII) (1:100; eBiosciences), phycoerythrin (PE)-conjugated anti-inducible nitric oxide synthase (iNOS) (1:20; Santa Cruz Biotechnology), and PE-conjugated anti-COX2 (1:20; Santa Cruz Biotechnology). For the intracellular detection of iNOS and COX-2, cells were permeabilized in a solution containing 1% paraformaldehyde (PFA), 0.1% saponin (Sigma-Aldrich), and 10 mM HEPES for 30 min at room temperature. Cells were then washed with PBS and stained with either one of the fluorescently conjugated primary antibodies for an additional 30 min on ice. For all multicolor experiments, fluorescence-minus-one (FMO) staining was used to define the cutoff for positivity.

Tissue processing and histology. Spinal cords were collected and prepared as described previously (Pineau and Lacroix, 2007). Briefly, mice were overdosed with a mixture of ketamine–xylazine and transcardially perfused with 4% PFA, pH 7.4, in PBS. Spinal cords were dissected out and placed overnight in a PBS/20% sucrose solution. For each animal, a spinal cord segment of 12 mm centered over the lesion site was cut in several series of 14-μm-thick coronal sections using a cryostat. For immunohistochemistry against 7/4, mice were perfused with 0.9% saline solution, followed by 4% PFA, pH 9.5, in borax buffer. Spinal cords were dissected out, postfixed for 2 d, and placed overnight in a 4% PFA–borax/10% sucrose solution until processing using a cryostat set at 30 μm thickness. All sections were collected directly onto slides having a permanent positively charged surface (Surgipath Canada) and stored at −20°C until use. To identify the lesion epicenter and quantify lesion volume, one series of adjacent sections was stained with hematoxylin–eosin (H&E) and luxol fast blue (LFB).

Immunohistochemistry and quantification of immunolabeling. Cells expressing $P2X_4$ in the normal and injured spinal cord were identified by confocal immunofluorescence labeling of the reporter protein β-galactosidase (β-Gal; 1:20,000; MP Biomedicals), HuC/HuD (to visualize neurons; 1:80; Invitrogen), NeuN (neurons; 1:250; Millipore), GFAP (astrocytes; 1:100; Invitrogen), and CD11b (microglia/macrophages; 1:500; AbD Serotec). Alexa Fluor secondary antibody conjugates (1:200; Invitrogen) were used as secondary antibodies, whereas 4′, 6-diamidino-2-phenylindole, dilactate (Invitrogen) was used for nuclear counterstaining. Immunofluorescence labeling was performed according to our previously published methods (Barrette et al., 2008). Sections were observed and imaged on a Fluoview FV1000 confocal microscope system equipped with argon 488, helium–neon-1 543, and helium–neon-2 633 lasers (Olympus).

Immunoperoxidase labeling using the anti-7/4 antibody was performed to detect both neutrophils and proinflammatory M1 macrophages in the spinal cord of injured mice. Immunoperoxidase labeling was performed on spinal cord tissue sections directly mounted onto slides using CoverWell incubation chambers (Invitrogen) and our previously published protocol (Pineau and Lacroix, 2007), with the only difference that sections were pretreated for 15 min with proteinase K to improve immunolabeling efficiency. The anti-7/4 antibody was purchased from AbD Serotec and used at a dilution of 1:800. After immunoperoxidase labeling, tissue sections were counterstained with LFB to visualize damaged areas.

For the quantification of neutrophils and M1 macrophages, the outline of the coronal section was traced at 20× magnification, and a grid of 50 $\times$ 50 μm was positioned over the spinal cord using the Bioquant Nova Prime software (Bioquant Image Analysis Corporation). All $7/4^{+}$ cells were then counted at 20× magnification. Results were expressed as an average number of positive cells per coronal section.

Macrophage and microglial activity in the injured mouse spinal cord was examined using the anti-galectin-3 (Gal-3; also referred to as Mac-2) antibody (1:500; American Type Culture Collection), as described in previous studies (Reichert and Rotshenker, 1999; Kriz et al., 2003; Lalancette-Hebert et al., 2007). For the quantification, the proportional area of tissue occupied by Gal-3 immunoperoxidase labeling was measured in coronal sections taken at specific distances from the lesion epicenter. In brief, digital images were collected with a high-resolution Retiga QICAM fast color 1394 camera (1392 $\times$ 1040 pixels; QImaging) installed on a Nikon Eclipse 80i microscope. Digitized images were then thresholded using the Bioquant Nova Prime software, such that only immunoperoxidase-labeled product resulted in measurable pixels, and the area occupied by the signal was measured and divided by the total area of the cross-section.

All quantifications were done blind with respect to the identity of the animals, and the epineurial layer was excluded from analyses.

Lesion volume analysis. For calculating areas of tissue damage and lesion volume after SCI, five coronal sections with easily identifiable anatomical landmarks were chosen for morphometric study. Briefly, a 12 mm segment of spinal cord encompassing the injury site was fixed in PFA ($n = 5$ animals per group), transverse sectioned at 14 μm, and then stained with H&E and LFB for gray and white matter visualization. Sections spaced at every 390 μm were used for analysis of injured white and gray matter using computer-assisted microscopy and Neurolucida software (MicroBrightField). In each section, the total area of the cord segment was first determined. Damaged white and gray matter areas were determined. Tissue was characterized as damaged by the presence of infiltrating immune cells, myelin breakdown, shrunken eosinophilic neurons, and hemorrhage. The areas of each section was calculated by Neurolucida software and then summated for the volumes of each spinal cord.

Behavioral analyses. Recovery of locomotor function after SCI was quantified in an open field using the Basso Mouse Scale (BMS), according to the method developed by Basso et al. (2006). Recovery of hindlimb function was also assessed using the grip walk (GW) test, a modified version of the grid walk or "foot fault" test, following the method recently described by Pajooheish-Ganji et al. (2010). All behavioral analyses were done blind with respect to the identity of the animals.

Statistical analysis. Statistical evaluations were performed with one- or two-way ANOVA or repeated-measures ANOVA. Post-ANOVA comparisons were made using the Bonferroni's correction. All statistical analyses were performed using the GraphPad Prism software (GraphPad Software). A p value <0.05 was considered as statistically significant.

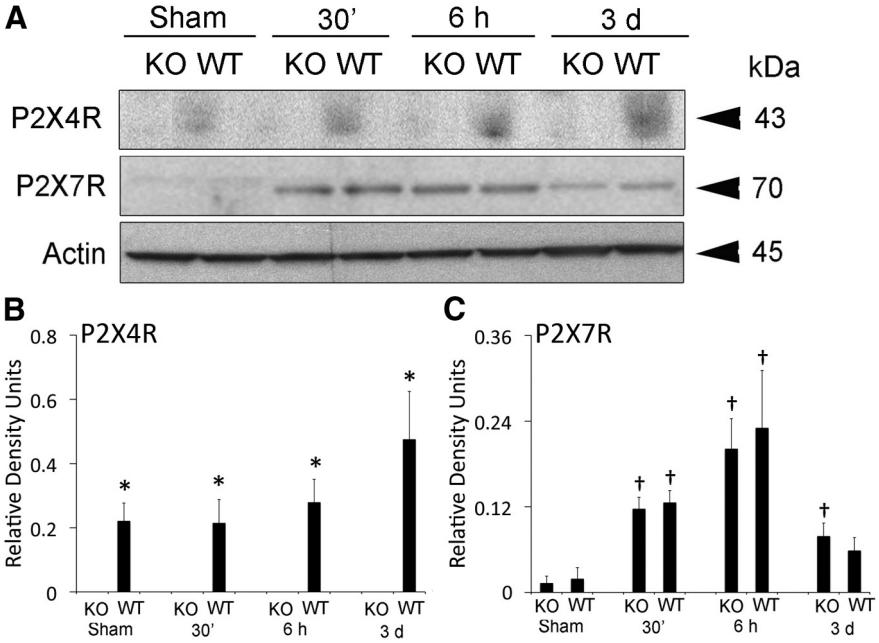

Figure 1. $P2X_4$ and $P2X_7$ expression in the normal and injured mouse spinal cord. ***A***, Representative immunoblots of $P2X_4$ and $P2X_7$ receptor expression after SCI. ***B***, Densitometric analysis indicates that $P2X_4$ protein expression is increased after SCI. The $P2X_4$ protein was not detected in $P2X_4$-KO mice. ***C***, $P2X_7$ expression is not altered in $P2X_4$-KO animals when compared with WT animals. Moreover, the levels of $P2X_7$ increased at 6 h after SCI ($n = 5$ per group). Data are presented as mean ± SEM. $^*p < 0.05$ compared with $P2X_4$-KO animals. $^\dagger p < 0.05$ compared with sham animals.

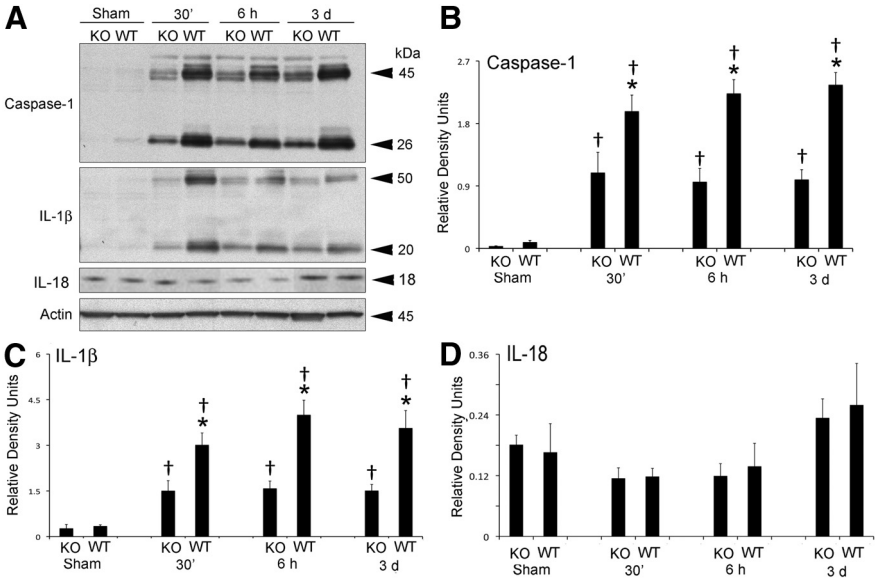

Figure 2. Increased expression of bioactive caspase-1 and IL-1β is reduced in the injured spinal cord of $P2X_4$-KO mice. ***A***, Representative immunoblots of caspase-1, IL-1β, and IL-18 after SCI. ***B–D***, Densitometric analysis indicates that both caspase-1 (***B***) and IL-1β (***C***) are decreased in the $P2X_4$-KO when compared with WT animals. Levels of IL-18 (***D***) are not altered in $P2X_4$-KO animals when compared with WT animals ($n = 5$ per group). Data are presented as mean ± SEM. $^*p < 0.05$ compared with $P2X_4$-KO animals. $^\dagger p < 0.05$ compared with sham animals.

Results

Caspase-1 and IL-1β responses are decreased in $P2X_4$-KO mice after SCI

$P2X_4$ and $P2X_7$ receptor expression in the spinal cord was analyzed by immunoblotting in WT and $P2X_4$-KO mice at 30 min, 6 h, and 3 d after SCI (Fig. 1). Three days after SCI, $P2X_4$ expression was significantly elevated in WT animals, whereas $P2X_4$ was not detected in $P2X_4$-KO mice, thus corroborating that the KO phenotype was maintained in this colony of animals. However, although SCI significantly increased levels of $P2X_7$ by 6 h after SCI, no significant differences in $P2X_7$ expression were observed between WT and $P2X_4$-KO mice (Fig. 1). As shown in Figure 2, active caspase-1 and IL-1β were elevated after SCI in both WT and KO mice after SCI, but the levels of these proteins were significantly higher in WT animals when compared with $P2X_4$-KO mice. In contrast, levels of active IL-18 were not significantly altered after SCI in either WT or $P2X_4$-KO mice. These results indicate that $P2X_4$ is involved in inflammasome activation after SCI.

$P2X_4$ is expressed in neurons of the dorsal horn and medial gray

To investigate which cell type(s) express $P2X_4$ in the normal and injured mouse spinal cord, we took advantage of the fact that the

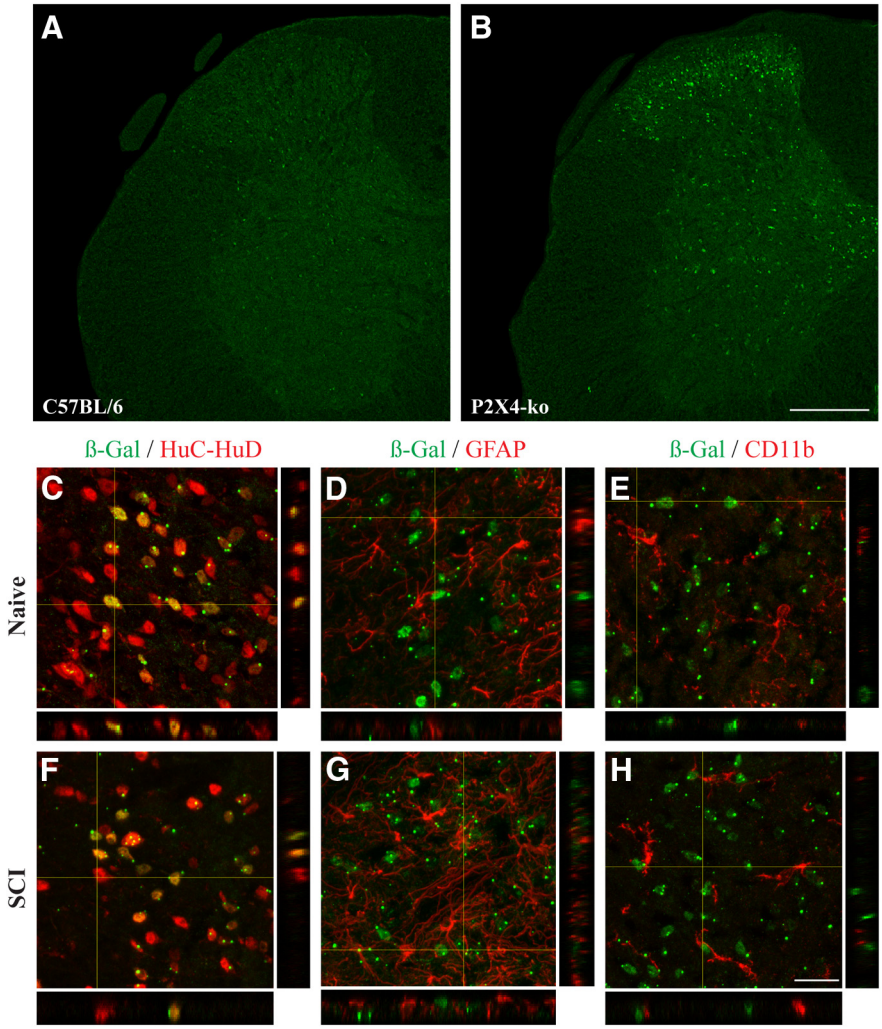

Figure 3. β-Gal staining is localized in neurons in the normal and injured spinal cord of $P2X_4$-KO mice. ***A***, ***B***, Representative confocal photomicrographs showing β-Gal immunostaining (green) in the spinal cord of naive C57BL/6 (negative control) and $P2X_4$-KO mice. Note that, in $P2X_4$-KO mice, the β-Gal reporter gene was inserted in place of the first exon of $P2X_4$, meaning that the $P2X_4$ promoter drives expression of β-Gal in these animals. ***C–E***, β-Gal immunoreactivity colocalized with the neuronal marker HuC/HuD (red, ***C***) but not with GFAP-immunoreactive astrocytes (red, ***D***) and CD11b-immunoreactive microglia (red, ***E***), in the spinal cord dorsal horn of naive $P2X_4$-KO mice. ***F–H***, β-Gal expression colocalized with neurons, but not astrocytes and microglia, at 24 h after SCI. Scale bars: (in ***B***) ***A***, ***B***, 200 μm; (in ***H***) ***C–H***, 20 μm.

reporter gene β-Gal was inserted in place of the first exon of $P2X_4$ in $P2X_4$-KO animals. β-Gal expression in the mouse spinal cord was examined using multiple immunofluorescence confocal microscopy. As demonstrated in Figure 3, no β-Gal signal was detected in the spinal cord of C57BL/6 (negative control) mice. In contrast, β-Gal immunostaining was clearly detected in the spinal cord of $P2X_4$-KO mice, with expression mainly located in the dorsal horn and medial gray areas. Combination of β-Gal immunostaining with immunofluorescence markers of neurons (HuC/HuD), astrocytes (GFAP), and microglia (CD11b) revealed that mostly all β-Gal$^+$ cells also expressed the neuronal marker HuC/HuD (Fig. 3*C–E*). Importantly, neurons were found to be the main, if not the only, cell type expressing β-Gal in both the normal and injured mouse spinal cord (Fig. 3*F–H*). This expression pattern was observed until at least day 3 after SCI, the latest time point examined in colocalization experiments. These findings were confirmed using a second antibody specific for neurons, NeuN (data not shown).

$P2X_4$ deficiency in neural cells reduces inflammation at sites of SCI

To establish whether the anti-7/4 antibody may be appropriate for analysis of infiltration of neutrophils and monocyte-derived M1 macrophages using immunohistochemistry, we first confirmed that the 7/4 antigen [also referred to as Ly-6B (Rosas et al., 2010)] was expressed in these two subsets of infiltrating myeloid cells but that it was not present in activated resident microglia. To accomplish this aim, we used flow cytometry, which allows simultaneous analysis of several different markers in individual cells in a quantitative manner. Additionally, this approach took advantage of the fact that infiltrating blood-derived leukocytes and microglia express different levels (high vs dim) of the leukocyte common antigen CD45 (Sedgwick et al., 1991; Babcock et al., 2003). As shown in Figure 4*A*, CD45^{hi} CD11b$^+$ Ly-6C$^+$ Ly-6G$^+$ neutrophils and CD45^{hi} CD11b$^+$ Ly-6C^{hi} Ly-6G$^-$ monocyte-derived M1 macrophages expressed 7/4 at high intensity, whereas the 7/4 antigen was absent in CD45^{dim} CD11b$^+$ Ly-6C$^-$ Ly-6G$^-$ microglia.

To determine whether deficiency in $P2X_4$ affects the immune cell infiltration at the injury site, we next quantified the number of neutrophils and proinflammatory M1 macrophages identified by 7/4 immunolabeling in tissue sections from $P2X_4$-KO and WT mice (Fig. 4*B–D*). At 12 h after SCI, ~1123 ± 72 cells expressing the 7/4 marker were counted at the lesion epicenter in WT mice. This number was reduced by ~25% in $P2X_4$-KO mice, with an average of 855 ± 77 7/4$^+$ cells at the lesion epicenter. This effect was transient, and the numbers of 7/4$^+$ cells at the lesion epicenter were not significantly different (ANOVA) between the two groups at 4 d after SCI (data not shown).

To confirm that $P2X_4$ channels expressed in neural cells (as opposed to in bone marrow-derived leukocytes) were involved in the initiation of neuroinflammation after SCI, we investigated immune cell recruitment in irradiation bone marrow chimeras. First, we confirmed that irradiation did not lead to the infiltration of 7/4$^+$ cells in the spinal cord of non-injured, laminectomized chimeric mice (Fig. 4*E*). However, the pattern of expression was dramatically different after SCI in which 7/4$^+$ cells were observed within the perivascular spaces of spinal cord blood vessels as early as 6 h (Fig. 4*F*). At 12 h after SCI, WT mice that were reconstituted with either WT (WT → WT) or $P2X_4$-deficient (P2X4-KO → WT) bone marrow did not show a significant reduction in recruitment of 7/4$^+$ neutrophils and monocyte-derived M1 macrophages (Fig. 4*G*). In contrast, $P2X_4$-KO mice reconstituted with WT bone marrow (WT → $P2X_4$-KO) had markedly reduced immune cell infiltration at the injury site. These results confirm that $P2X_4$ plays an important role in neural cells but not in bone marrow-derived cells, in the regulation of innate immune cell

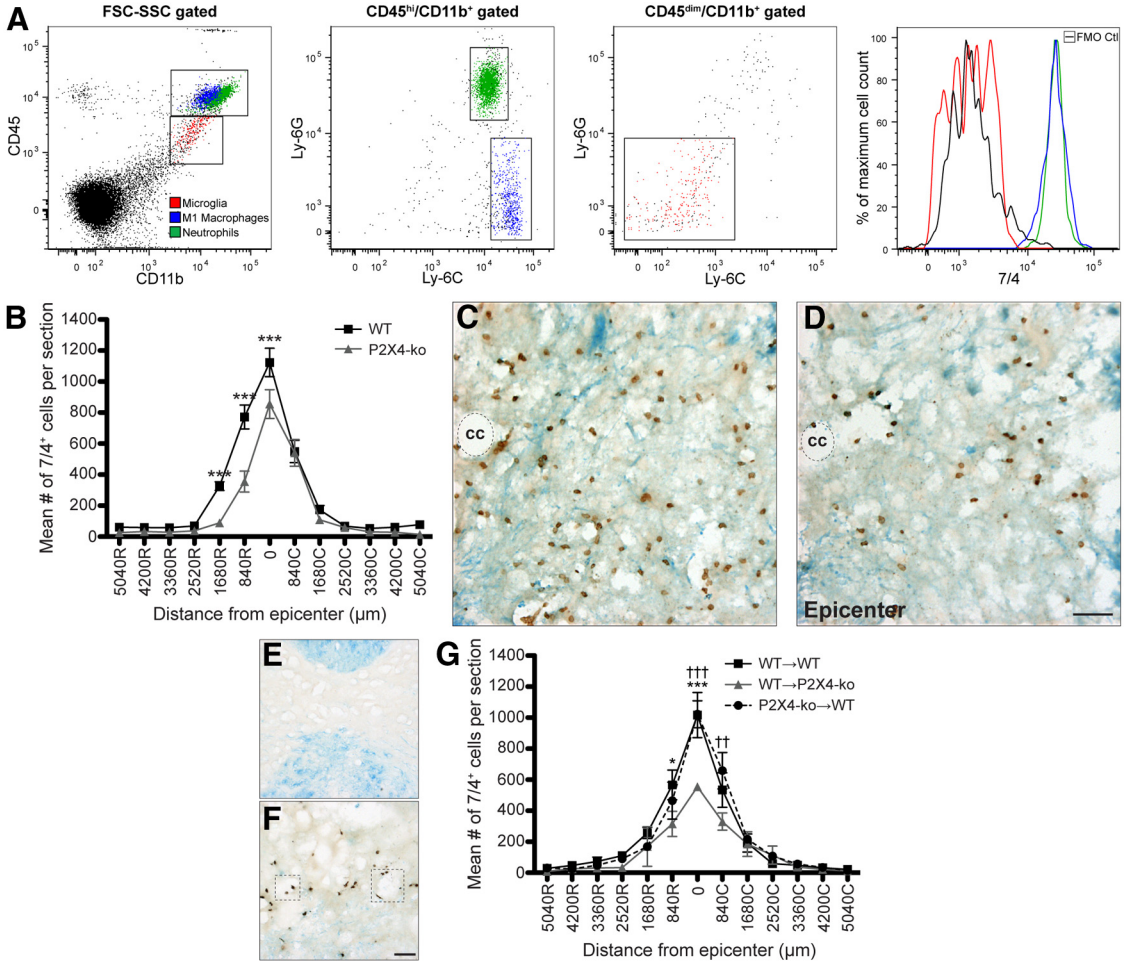

Figure 4. $P2X_4$ deficiency in neural cells reduces neutrophil and M1 macrophage infiltration at sites of SCI. ***A***, Evaluation of 7/4 as a specific marker for blood-derived neutrophils and M1 macrophages. Expression of 7/4 in neutrophils (green; $CD45^{hi}CD11b^{+}$ Ly-$6C^{+}$ Ly-$6G^{+}$), M1 macrophages (blue; $CD45^{hi}CD11b^{+}$ Ly-$6C^{hi}$ Ly-$6G^{-}$), and microglia (red; $CD45^{dim}CD11b^{+}$ Ly-$6C^{-}$ Ly-$6G^{-}$) isolated by flow cytometry from the spinal cord of a C57BL/6 mouse at 12 h after SCI (data are representative of $n = 6$ mice). The FMO negative control for 7/4 (i.e., all antibodies minus the PE-conjugated anti-7/4 antibody; $CD45^{+}CD11b^{+}$-gated cells) is shown in the far right. ***B***, Quantification of the number of neutrophils and proinflammatory M1 macrophages, as visualized by immunostaining of the 7/4 antigen, at various rostral (R) and caudal (C) distances from the lesion epicenter at 12 h after SCI ($n = 9$–11 per group). ***C***, ***D***, Representative bright-field photomicrographs showing 7/4 immunolabeling in the spinal cord of WT (***C***) and $P2X_4$-KO (***D***) mice at 12 h after SCI. The central canal (cc) in ***C*** and ***D*** is identified by dashed lines. ***E***, Representative bright-field photomicrograph showing the absence of $7/4^{+}$ cells in the spinal cord of a non-injured WT → WT chimeric mouse at 12 h after laminectomy. ***F***, Photomicrograph showing several $7/4^{+}$ cells closely associated with spinal cord blood vessels in a WT → WT chimeric mouse at 6 h after SCI. Dashed boxes delimit blood vessels. ***G***, Quantification of $7/4^{+}$ neutrophils and M1 macrophages in the spinal cord of WT → WT, WT → $P2X_4$-KO, and $P2X_4$-KO → WT bone marrow chimeras at 12 h after SCI ($n = 4$ per group). $^{*}p < 0.05$, $^{**}p < 0.01$, and $^{***}p < 0.001$, significant difference between WT and $P2X_4$-KO mice (***B***). $^{*}p < 0.05$, $^{**}p < 0.01$, and $^{***}p < 0.001$, significant difference between WT → WT and WT → $P2X_4$-KO chimeric mice (***G***). $^{\dagger}p < 0.05$, $^{\dagger\dagger}p < 0.01$, and $^{\dagger\dagger\dagger}p < 0.001$, significant difference between $P2X_4$-KO → WT and WT → $P2X_4$-KO chimeric mice (***G***). Scale bars: (in ***D***) ***C***, ***D***, 50 μm; (in ***F***) ***E***, ***F***, 50 μm.

infiltration at sites of SCI. Importantly, this conclusion would not have been affected even if irradiation would have promoted the infiltration of bone marrow-derived leukocytes in the spinal cord, as was suggested by others (Shechter et al., 2009; Donnelly et al., 2011).

Using immunohistochemistry against Gal-3, we next examined microglial/macrophage activation and found that it was reduced by ~50% in the spinal cord of $P2X_4$-KO mice compared with WT mice at 4 d after SCI (Fig. 5*A–C*). In contrast, these differences were not observed at 38 d (data not shown). To further explore the role of $P2X_4$ in the response of microglia and infiltrating macrophages, referred hereinafter as monocyte-derived macrophages (Kigerl et al., 2009; Shechter et al., 2009), cells were isolated from the injured spinal cord at 7 and 14 d and then characterized and quantified by flow cytometry based on expression of the following markers: CD45, CD11b, Ly-6C, MHCII, CD11c, iNOS, and COX-2. As shown in Figure 5, *D* and *E*, no significant changes in numbers of monocyte-derived M1 macrophages ($CD45^{hi}CD11b^{+}$ Ly-$6C^{hi}$), monocyte-derived M2 macrophages ($CD45^{hi}CD11b^{+}$ Ly-$6C^{-}$), and microglia ($CD45^{dim}CD11b^{+}$ Ly-$6C^{-}$) were detected between both groups at 7–14 d after SCI. With the exception of a modest, but significant, decrease in the number of $iNOS^{+}$ cells in the $P2X_4$ group at 7 d, no obvious differences were observed in the phenotype of microglia and macrophage subsets between both mouse strains. In agreement with Donnelly et al. (2011), iNOS was mainly detected in the $CD11b^{+}$/Ly-$6C^{-}$ population. Altogether, these results suggest that the immune response is attenuated and delayed in SCI $P2X_4$-KO mice, thus supporting a role of the inflammasome as an initiator of neuroinflammation after SCI.

$P2X_4$-KO mice show improved histopathological outcomes when compared with WT mice

To determine whether lack of $P2X_4$ expression resulted in decreased tissue damage after SCI *in vivo*, various groups of animals were subjected to SCI and killed 4 d after injury, and lesion vol-

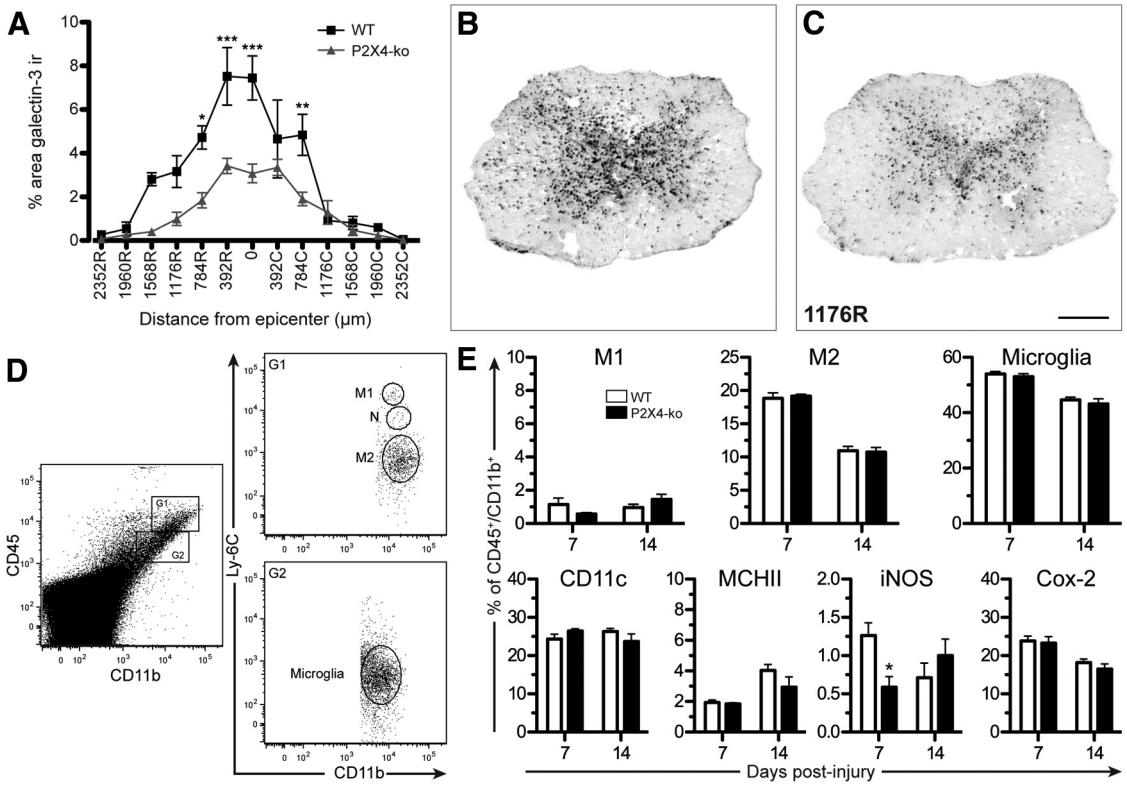

Figure 5. $P2X_4$ deficiency attenuates microglial/macrophage activation after SCI. ***A***, Quantification of microglial/macrophage activation, as visualized by Gal-3 immunolabeling, in the spinal cord of $P2X_4$-KO and WT mice at 4 d after SCI ($n = 5$ per group). ***B***, ***C***, Representative bright-field photomicrographs showing Gal-3 immunolabeling in the spinal cord of WT (***B***) and $P2X_4$-KO (***C***) mice at a distance of 1176 μm rostral to the lesion at 4 d after SCI. ***D***, Representative flow cytometry profiles showing the presence of monocyte-derived M1 macrophages (M1; $CD45^{hi}$ $CD11b^{+}$ Ly-$6C^{hi}$), monocyte-derived M2 macrophages (M2; $CD45^{hi}$ $CD11b^{+}$ Ly-$6C^{-}$), neutrophils (N; $CD45^{hi}$ $CD11b^{+}$ Ly-$6C^{+}$), and microglia ($CD45^{dim}$ $CD11b^{+}$ Ly-$6C^{-}$) in the spinal cord of a C57BL/6 mouse at 7 d after SCI (representative of $n = 6$ mice per group per time point). CD45 levels (high vs intermediate) were used to distinguish infiltrating blood-derived $CD11b^{+}$ myeloid cells ($CD45^{hi}$ $CD11b^{+}$; boxed region G1) from $CD11b^{+}$ resident microglia ($CD45^{dim}$ $CD11b^{+}$; boxed region G2). ***E***, Quantification of proportions of M1 macrophages, M2 macrophages, and microglia, relative to total $CD45^{+}$ $CD11b^{+}$ myeloid cells, in $P2X_4$-KO and WT mice at 7 and 14 d after SCI. Also shown in ***E*** are quantitative analyses of CD11c, MHCII, iNOS, and COX-2 expression. $^{*}p < 0.05$, $^{**}p < 0.01$, and $^{***}p < 0.001$, significant difference between WT and $P2X_4$-KO mice (***A***, ***E***). Scale bar: (in ***C***) ***B***, ***C***, 250 μm.

ume was measured. Spinal cord sections from $P2X_4$-KO mice showed a significant reduction in lesion volume after SCI when compared with injured WT mice (Fig. 6*A*), as determined by decreased immune cell infiltration, diminished white matter degeneration, and preservation of motor neuron morphology. These results are consistent with the lower levels of inflammasome activation and decrease in IL-1β cytokine production observed in $P2X_4$-KO mice.

Functional recovery after SCI is improved in $P2X_4$-KO mice when compared with WT mice

We next examined whether deletion of the $P2X_4$ gene affects locomotor recovery after SCI. Evaluation was performed in an open field using the 9-point BMS scale and the 11-point BMS subscores. Uninjured $P2X_4$-KO and WT (C57BL/6) mice performed flawlessly in these tests and received perfect scores on the BMS and BMS subscore scales. However, after a moderate (50 kdyn) traumatic SCI (Fig. 6*B*), $P2X_4$-KO mice performed significantly better than WT mice at 1 and 3 d after SCI. At 3 d after SCI, >80% of $P2X_4$-KO mice regained occasional plantar stepping (score ≥ 4 on the BMS) compared with only 30% in control mice. Importantly, significant improvements in specific aspects of locomotion, such as coordination, paw position, and trunk stability, were observed between $P2X_4$-KO mice (average subscore of 6.8 ± 0.5 at 35 d after SCI) and WT mice (5.0 ± 0.4) at the conclusion of behavioral testing (Fig. 6*C*). Early recovery of forelimb–hindlimb coordination after SCI was confirmed in $P2X_4$-KO mice compared with WT mice using the GW test (Fig. 6*D*). The severity of SCI was almost identical between both groups, with an average force applied of 51.9 ± 0.8 kdyn for WT mice versus 51.9 ± 0.7 kdyn for $P2X_4$-KO mice (Fig. 6*E*). Moreover, the average spinal cord tissue displacement did not differ significantly (ANOVA) between groups, with 357.6 ± 12.6 μm for WT mice compared with 392.5 ± 17.4 μm for $P2X_4$-KO mice. Thus, lack of expression of $P2X_4$ results in improved behavioral outcomes after SCI.

Discussion

In this study, we show that deletion of $P2X_4$ in mice results in decreased innate immune responses after SCI compared with WT animals. These decreased inflammatory responses involve a significant reduction in inflammasome activation in neurons as determined by decreased cleavage of caspase-1 and production of IL-1β and decreased infiltration of innate immune cells into the injury site acutely after SCI. The reduction in inflammatory processes was transient in nature but resulted in significant improvements in histopathological and functional outcomes. Our findings suggest that blocking neuronal $P2X_4$ acutely after SCI may be an effective means to prevent the detrimental effects of inflammation and loss of neurological function after trauma.

To investigate which CNS cell type(s) express $P2X_4$ in the normal and injured mouse spinal cord, we took advantage of the

finding that the $P2X_4$ promoter drives β-Gal expression in $P2X_4$-KO animals. This approach also served to get around the difficult problem that all commercially available anti-$P2X_4$ antibodies tested produced positive immunostaining in spinal cord tissue from $P2X_4$-KO mice (de Rivero Vaccari JP, Keane RW, unpublished observations). Therefore, commercial antibodies were not reliable for detection of $P2X_4$ immunoreactivity in the mouse CNS, but rather β-Gal immunodetection proved to better measure of $P2X_4$ cell-type expression. Our results demonstrate that the colocalization of β-Gal immunostaining was almost exclusively observed within neurons and not astrocytes or microglia. Thus, in both the normal and injured spinal cord, $P2X_4$ is mainly expressed in neurons. However, our results do not rule out the possibility that cells that would normally express $P2X_4$ fail to infiltrate in the spinal cord, either in the control state or after SCI, because of the lack of the receptor. In this case, such cells would not be seen in KO animals, despite their possible relevance to outcome.

We have shown previously that the NOD-like receptor complex NLRP1 inflammasome is expressed in neurons of the spinal cord. The NLRP1 inflammasome activates caspase-1, resulting in production of IL-1β and IL-18 (de Rivero Vaccari et al., 2008). In this study, animals lacking $P2X_4$ showed lower levels of inflammasome activation as determined by decreased levels of active caspase-1 and IL-1β. However, the levels of IL-18 did not significantly differ between WT animals and KOs. This finding suggests that IL-1β and IL-18 are regulated by different signaling mechanisms after SCI. In support of this idea are reports demonstrating that, in addition to regulation by the inflammasome, IL-18 levels are influenced by exogenous hormones (Park et al., 2005a,b, 2007).

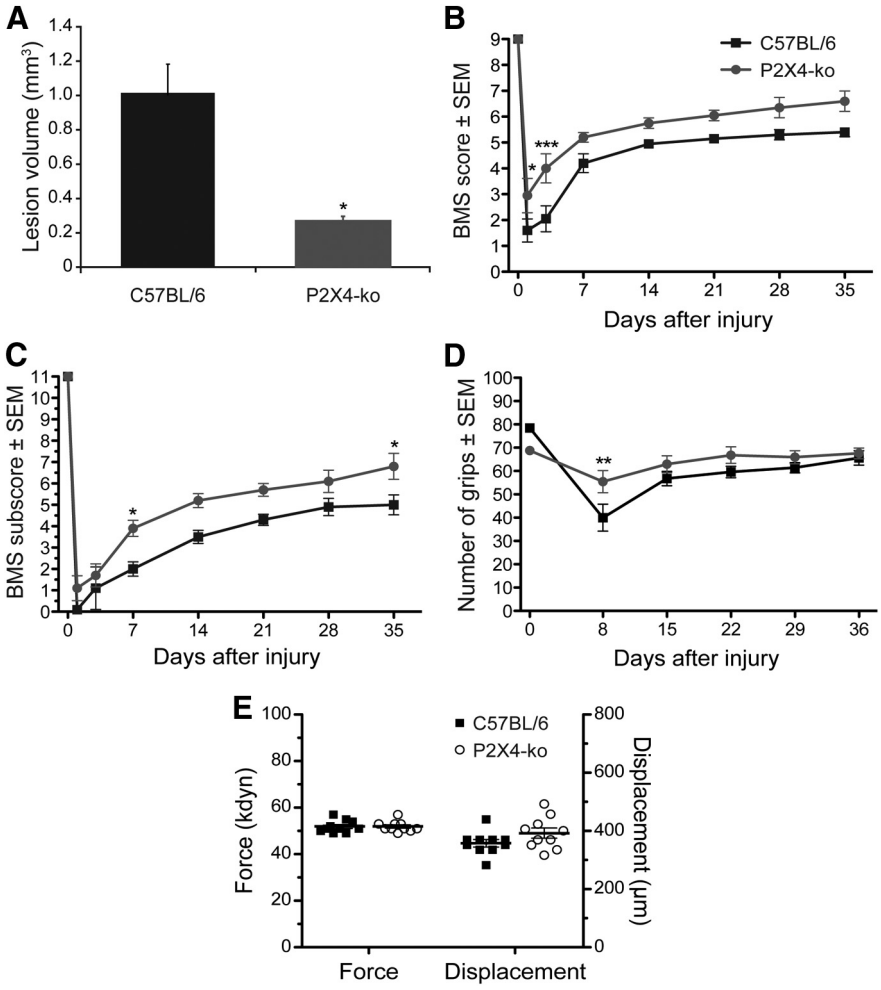

Figure 6. Spinal cord lesion volume and recovery of locomotor function are improved in $P2X_4$-KO mice. ***A***, $P2X_4$-KO mice had significantly reduced spinal cord tissue damage at 4 d after injury ($n = 5$ per group). ***B***, ***C***, Locomotor function was assessed using the BMS (***B***) and BMS subscore (***C***) over a 35 d period after SCI ($n = 10$ mice per group). ***D***, The modified GW test was also used to assess hindpaw function, and the number of hindpaw grips on the GW counted at 8, 15, 22, 29, and 36 d after injury ($n = 10$ mice per group). The GW test was performed using three different patterns: easy, medium, and hard. The total number of grips for the three different patterns is presented in ***D***. ***E***, Impact force (in kilodynes) and spinal cord tissue displacement (in micrometers) at the time of the contusion injury for all animals included in behavioral analyses. $^*p < 0.05$, $^{**}p < 0.01$, and $^{***}p < 0.001$ compared with SCI WT (C57BL/6) mice; two-way repeated-measures ANOVA, Bonferroni's *post hoc* test.

$P2X_4$ forms heteromeric interactions with another purinergic receptor, $P2X_7$ (Guo et al., 2007). In the present study, the protein expression levels of $P2X_7$ were not affected in the $P2X_4$-KO mice after SCI, suggesting that $P2X_4$ is not necessary for the regulation of $P2X_7$ in the spinal cord. However, $P2X_7$ is an ATP-activated receptor involved in the inflammatory response after SCI (Wang et al., 2004; Peng et al., 2009). Moreover, $P2X_7$ interacts with pannexin-1 and the inflammasome in CNS cells (Silverman et al., 2009). Therefore, more detailed studies involving protein associations of $P2X_4$ and $P2X_7$ with inflammasomes are needed to establish more precise regulation of inflammasome responses after SCI.

Deletion of $P2X_4$ also significantly diminished the number of neutrophils and monocyte-derived M1 macrophages that infiltrated the injury site after SCI. $P2X_4$-KO animals showed a 25% decrease in the amount of infiltrated neutrophils and M1 macrophages in the spinal cord at 12 h after injury and a 50% decrease in the amount of microglial/macrophage activation at 4 d. Importantly, studies using irradiation bone marrow chimeras revealed that the $P2X_4$ was required on radioresistant (i.e., non-bone marrow-derived) but not radiosensitive (i.e., bone marrow-derived) host cells for modulating innate immune cell entry into the damaged spinal cord. Together with our previous work that showed that the IL-1R1/MyD88 signaling pathway triggers innate immune cell infiltration after SCI (Pineau et al., 2010), these results suggest that one of the cellular sources of IL-1β in the injured spinal cord are neurons and that activation of $P2X_4$ is critical for inflammatory cell infiltration. The relationship between inflammation and the pathogenesis of SCI remains controversial in that mounting evidence shows that some subsets of immune cells may support regeneration, whereas others may cause neurotoxicity (Gensel et al., 2009; Kigerl et al., 2009; Stirling et al., 2009). A recent cell depletion study has demonstrated quite convincingly that preventing the recruitment of both neutrophils and monocytes that differentiate into proinflammatory M1 macrophages is beneficial for functional recovery after injury (Lee et al., 2011).

Previous reports have mainly discussed the effects of ATP stimulation of $P2X_4$ that results in increased intracellular calcium concentrations, activation of mitogen-activated protein kinases, and release of proinflammatory cytokines (Ferrari et al., 1997; Schwiebert et al., 2002). $P2X_4$ receptor activation has been suggested to mediate synaptic transmission (North, 2002), and $P2X_4$ signaling may play a critical role in the inflammatory responses in the pathology of brain tumors, neuropathic pain, and multiple sclerosis (Guo et al., 2004, 2006; Guo and Schluesener, 2005; Ulmann et al., 2008). Our study shows that $P2X_4$-KO animals have lower levels of caspase-1 activation and IL-1β cleavage, resulting in significant improvement in tissue sparing and functional recovery. The improvements in functional outcomes were predominantly observed during the first week after injury, suggesting that the deleterious inflammatory processes mediated by $P2X_4$ activation occur during the acute phase after SCI. Interestingly, only neurons were found to express $P2X_4$ in the spinal cord during the acute phase after SCI. However, other groups have reported that activated microglia in the spinal cord upregulate $P2X_4$ expression after peripheral (sciatic) nerve injury, although the increased expression peaked during the second week after lesion in this particular model (Cavaliere et al., 2003; Tsuda et al., 2003; Schwab et al., 2005; Ulmann et al., 2008). In the chronic phase after SCI, $P2X_4$ does not seem to play a significant role, yet the improved functional recovery observed in $P2X_4$-KO compared with WT mice was maintained up to at least day 35. We propose that blocking neuronal $P2X_4$ early after SCI may be an effective means for preventing the detrimental effects of inflammation and loss of neurological function in a variety of CNS injuries, including traumatic brain injury, ischemia, and SCI.

References

Auffray C, Fogg D, Garfa M, Elain G, Join-Lambert O, Kayal S, Sarnacki S, Cumano A, Lauvau G, Geissmann F (2007) Monitoring of blood vessels and tissues by a population of monocytes with patrolling behavior. Science 317:666–670.

Babcock AA, Kuziel WA, Rivest S, Owens T (2003) Chemokine expression by glial cells directs leukocytes to sites of axonal injury in the CNS. J Neurosci 23:7922–7930.

Barrette B, Hébert MA, Filali M, Lafortune K, Vallières N, Gowing G, Julien JP, Lacroix S (2008) Requirement of myeloid cells for axon regeneration. J Neurosci 28:9363–9376.

Basso DM, Fisher LC, Anderson AJ, Jakeman LB, McTigue DM, Popovich PG (2006) Basso Mouse Scale for locomotion detects differences in recovery after spinal cord injury in five common mouse strains. J Neurotrauma 23:635–659.

Buell G, Lewis C, Collo G, North RA, Surprenant A (1996) An antagonist-insensitive P2X receptor expressed in epithelia and brain. EMBO J 15:55–62.

Burnstock G (2007) Physiology and pathophysiology of purinergic neurotransmission. Physiol Rev 87:659–797.

Casas-Pruneda G, Reyes JP, Pérez-Flores G, Pérez-Cornejo P, Arreola J (2009) Functional interactions between P2X4 and P2X7 receptors from mouse salivary epithelia. J Physiol 587:2887–2901.

Cavaliere F, Florenzano F, Amadio S, Fusco FR, Viscomi MT, D'Ambrosi N, Vacca F, Sancesario G, Bernardi G, Molinari M, Volonté C (2003) Up-regulation of P2X2, P2X4 receptor and ischemic cell death: prevention by P2 antagonists. Neuroscience 120:85–98.

Coull JA, Beggs S, Boudreau D, Boivin D, Tsuda M, Inoue K, Gravel C, Salter MW, De Koninck Y (2005) BDNF from microglia causes the shift in neuronal anion gradient underlying neuropathic pain. Nature 438:1017–1021.

de Rivero Vaccari JP, Lotocki G, Marcillo AE, Dietrich WD, Keane RW (2008) A molecular platform in neurons regulates inflammation after spinal cord injury. J Neurosci 28:3404–3414.

Donnelly DJ, Longbrake EE, Shawler TM, Kigerl KA, Lai W, Tovar CA, Ransohoff RM, Popovich PG (2011) Deficient CX3CR1 signaling promotes recovery after mouse spinal cord injury by limiting the recruitment and activation of Ly6Clo/iNOS$^+$ macrophages. J Neurosci 31:9910–9922.

Ferrari D, Chiozzi P, Falzoni S, Dal Susino M, Melchiorri L, Baricordi OR, Di Virgilio F (1997) Extracellular ATP triggers IL-1 beta release by activating the purinergic P2Z receptor of human macrophages. J Immunol 159:1451–1458.

Gensel JC, Nakamura S, Guan Z, van Rooijen N, Ankeny DP, Popovich PG (2009) Macrophages promote axon regeneration with concurrent neurotoxicity. J Neurosci 29:3956–3968.

Gordon S, Taylor PR (2005) Monocyte and macrophage heterogeneity. Nat Rev Immunol 5:953–964.

Guo C, Masin M, Qureshi OS, Murrell-Lagnado RD (2007) Evidence for functional P2X4/P2X7 heteromeric receptors. Mol Pharmacol 72:1447–1456.

Guo LH, Schluesener HJ (2005) Lesional accumulation of $P2X_4$ receptor$^+$ macrophages in rat CNS during experimental autoimmune encephalomyelitis. Neuroscience 134:199–205.

Guo LH, Trautmann K, Schluesener HJ (2004) Expression of P2X4 receptor in rat C6 glioma by tumor-associated macrophages and activated microglia. J Neuroimmunol 152:67–72.

Guo LH, Guo KT, Wendel HP, Schluesener HJ (2006) Combinations of TLR and NOD2 ligands stimulate rat microglial P2X4R expression. Biochem Biophys Res Commun 349:1156–1162.

Kigerl KA, Gensel JC, Ankeny DP, Alexander JK, Donnelly DJ, Popovich PG (2009) Identification of two distinct macrophage subsets with divergent effects causing either neurotoxicity or regeneration in the injured mouse spinal cord. J Neurosci 29:13435–13444.

Kriz J, Gowing G, Julien JP (2003) Efficient three-drug cocktail for disease induced by mutant superoxide dismutase. Ann Neurol 53:429–436.

Lalancette-Hébert M, Gowing G, Simard A, Weng YC, Kriz J (2007) Selective ablation of proliferating microglial cells exacerbates ischemic injury in the brain. J Neurosci 27:2596–2605.

Lee SM, Rosen S, Weinstein P, van Rooijen N, Noble-Haeusslein LJ (2011) Prevention of both neutrophil and monocyte recruitment promotes recovery after spinal cord injury. J Neurotrauma 28:1893–1907.

Nadeau S, Filali M, Zhang J, Kerr BJ, Rivest S, Soulet D, Iwakura Y, de Rivero Vaccari JP, Keane RW, Lacroix S (2011) Functional recovery after peripheral nerve injury is dependent on the pro-inflammatory cytokines IL-1β and TNF: implications for neuropathic pain. J Neurosci 31:12533–12542.

Nahrendorf M, Swirski FK, Aikawa E, Stangenberg L, Wurdinger T, Figueiredo JL, Libby P, Weissleder R, Pittet MJ (2007) The healing myocardium sequentially mobilizes two monocyte subsets with divergent and complementary functions. J Exp Med 204:3037–3047.

North RA (2002) Molecular physiology of P2X receptors. Physiol Rev 82:1013–1067.

Pajoohesh-Ganji A, Byrnes KR, Fatemi G, Faden AI (2010) A combined scoring method to assess behavioral recovery after mouse spinal cord injury. Neurosci Res 67:117–125.

Park HJ, Kim HJ, Lee JH, Lee JY, Cho BK, Kang JS, Kang H, Yang Y, Cho DH (2005a) Corticotropin-releasing hormone (CRH) downregulates interleukin-18 expression in human HaCaT keratinocytes by activation of p38 mitogen-activated protein kinase (MAPK) pathway. J Invest Dermatol 124:751–755.

Park HS, Kim Y, Lee C (2005b) Single nucleotide variants in the beta2-adrenergic and beta3-adrenergic receptor genes explained 18.3% of adolescent obesity variation. J Hum Genet 50:365–369.

Park HJ, Kim HJ, Lee JY, Cho BK, Gallo RL, Cho DH (2007) Adrenocorticotropin hormone stimulates interleukin-18 expression in human HaCaT keratinocytes. J Invest Dermatol 127:1210–1216.

Peng W, Cotrina ML, Han X, Yu H, Bekar L, Blum L, Takano T, Tian GF, Goldman SA, Nedergaard M (2009) Systemic administration of an antagonist of the ATP-sensitive receptor P2X7 improves recovery after spinal cord injury. Proc Natl Acad Sci U S A 106:12489–12493.

Pineau I, Lacroix S (2007) Proinflammatory cytokine synthesis in the injured mouse spinal cord: multiphasic expression pattern and identification of the cell types involved. J Comp Neurol 500:267–285.

Pineau I, Sun L, Bastien D, Lacroix S (2010) Astrocytes initiate inflammation in the injured mouse spinal cord by promoting the entry of neutrophils and inflammatory monocytes in an IL-1 receptor/MyD88-dependent fashion. Brain Behav Immun 24:540–553.

Reichert F, Rotshenker S (1999) Galectin-3/MAC-2 in experimental allergic encephalomyelitis. Exp Neurol 160:508–514.

Rosas M, Thomas B, Stacey M, Gordon S, Taylor PR (2010) The myeloid 7/4-antigen defines recently generated inflammatory macrophages and is synonymous with Ly-6B. J Leukoc Biol 88:169–180.

Schwab JM, Guo L, Schluesener HJ (2005) Spinal cord injury induces early and persistent lesional P2X4 receptor expression. J Neuroimmunol 163:185–189.

Schwiebert LM, Rice WC, Kudlow BA, Taylor AL, Schwiebert EM (2002) Extracellular ATP signaling and P2X nucleotide receptors in monolayers of primary human vascular endothelial cells. Am J Physiol Cell Physiol 282:C289–C301.

Sedgwick JD, Schwender S, Imrich H, Dörries R, Butcher GW, ter Meulen V (1991) Isolation and direct characterization of resident microglial cells from the normal and inflamed central nervous system. Proc Natl Acad Sci U S A 88:7438–7442.

Shechter R, London A, Varol C, Raposo C, Cusimano M, Yovel G, Rolls A, Mack M, Pluchino S, Martino G, Jung S, Schwartz M (2009) Infiltrating blood-derived macrophages are vital cells playing an anti-inflammatory role in recovery from spinal cord injury in mice. PLoS Med 6:e1000113.

Silverman WR, de Rivero Vaccari JP, Locovei S, Qiu F, Carlsson SK, Scemes E, Keane RW, Dahl G (2009) The pannexin 1 channel activates the inflammasome in neurons and astrocytes. J Biol Chem 284:18143–18151.

Soto F, Garcia-Guzman M, Gomez-Hernandez JM, Hollmann M, Karschin C, Stühmer W (1996) P2X4: an ATP-activated ionotropic receptor cloned from rat brain. Proc Natl Acad Sci U S A 93:3684–3688.

Stirling DP, Liu S, Kubes P, Yong VW (2009) Depletion of Ly6G/Gr-1 leukocytes after spinal cord injury in mice alters wound healing and worsens neurological outcome. J Neurosci 29:753–764.

Tsuda M, Shigemoto-Mogami Y, Koizumi S, Mizokoshi A, Kohsaka S, Salter MW, Inoue K (2003) P2X4 receptors induced in spinal microglia gate tactile allodynia after nerve injury. Nature 424:778–783.

Ulmann L, Hatcher JP, Hughes JP, Chaumont S, Green PJ, Conquet F, Buell GN, Reeve AJ, Chessell IP, Rassendren F (2008) Upregulation of P2X4 receptors in spinal microglia after peripheral nerve injury mediates BDNF release and neuropathic pain. J Neurosci 28:11263–11268.

Wang X, Arcuino G, Takano T, Lin J, Peng WG, Wan P, Li P, Xu Q, Liu QS, Goldman SA, Nedergaard M (2004) P2X7 receptor inhibition improves recovery after spinal cord injury. Nat Med 10:821–827.

Weinhold K, Krause-Buchholz U, Rödel G, Kasper M, Barth K (2010) Interaction and interrelation of P2X7 and P2X4 receptor complexes in mouse lung epithelial cells. Cell Mol Life Sci 67:2631–2642.

Zhang Z, Artelt M, Burnet M, Trautmann K, Schluesener HJ (2006) Lesional accumulation of P2X4 receptor $^+$ monocytes following experimental traumatic brain injury. Exp Neurol 197:252–257.